Journal of Environmental Radioactivity 197 (2019) 109–115

Contents lists available at ScienceDirect

Journal of Environmental Radioactivity

journal homepage: www.elsevier.com/locate/jenvrad

Preliminary investigation of ^{222}Rn in the Yakumo Wind-hole, an algific talus deposits, from Izumo, southwest Honshu, Japan

Ritsuo Nomura[a,*], Mutsuo Inoue[b], Hisaki Kofuji[c]

[a] Geological Laboratory, Faculty of Education, Shimane University, and Shimane Peninsula and Shinjiko Nakaumi Estuary Geopark Promotion Conference, Matsue City Hall, Matsue, 690-8540, Japan

[b] Low Level Radioactivity Laboratory, Kanazawa University, Wake, Nomi, Ishikawa, 923-1224, Japan

[c] Mutsu Marine Laboratory, Japan Marine Science Foundation, Minato, Mutsu, Aomori, 035-0064, Japan

ARTICLE INFO

Keywords:
Radon
Wind-hole
Talus deposits
Seasonal variation
Convection
Relative humidity

ABSTRACT

The Yakumo Wind-hole in southwest Japan formed by landslip, and it is known as a cold air blowhole. This wind-hole consists of two parts, which have complementary relationships in regard to the flow of air, namely, topographically upper and lower holes that can be characterized as a warm wind-hole (WWH) and cold wind-hole (CWH), respectively. We carried out a preliminary investigation of radon behavior in the Yakumo Wind-hole. The data showed remarkable seasonal change from high ^{222}Rn concentrations reaching to 7.6 ± 0.1 kBq/m^3 in the warm season (mid-May to October) to low ^{222}Rn concentrations in the cold season (December to early May) at the CWH. The threshold in the regional atmospheric temperature was estimated as 16.2 °C for the beginning and 17.1 °C for the ending periods of air blow with higher ^{222}Rn concentrations. These seasonal changes in ^{222}Rn were not only associated with the dynamic convection caused by temperature differences in and out of the talus, but were also related to the relative humidity of air that is blown out. High ^{222}Rn concentrations were formed in the high humidity environment, and the humidity may possibly be associated with melting ice. According to the known information on ^{222}Rn behavior in relation to humidity, a radon trap in the growing ice in spring and in the melted water in summer are suggested. This study revealed that ^{222}Rn measurements are a useful tool to understand the air dynamics in the talus.

1. Introduction

A number of wind-holes, meaning holes formed in talus deposits from which cold air blows, exist at various locations in the Japanese Islands (Shimizu, 2004, 2015). Such an algific talus is called “fhuketsu” in Japanese, while “algific” comes from Latin *algificus*, which means “making cold” (Sawada, 2015). Blowing air is active when the temperature difference between the interior and exterior air becomes enhanced (Aratani, 1923, 1926; Egawa et al., 1980; Tanaka et al., 2000b, 2004; Sawada, 2015; Shimizu, 2015), and thus the cold air blows most strongly in summer. The Yakumo Wind-hole located in Izumo City, Shimane Prefecture, southwest Honshu, Japan, represents a seasonal wind-movement system in the talus. The air temperature of the cold wind-hole has been reported to be usually in the range of 5–6 °C in summer (Ogawa, 1996).

Most studies in Japan have hitherto focused on clarifying the air dynamics by measuring the temperature of the blowing air (Aratani, 1923, 1926; Shiboi, 1974; Egawa et al., 1980; Maki, 1998; Tanaka et al., 2000a, 2000b, 2004, 2006). Since the pioneering works of Aratani (1926) at the Nagahashiri Wind-hole in Akita Prefecture, northeast Honshu, the convection theory has been accepted. There are two holes at either end of a passage in the talus, and thus warm air drawn into the upper talus changes to cold air through the colder passage and blows out in the lower talus in summer. In contrast, cold air drawn into the lower slope changes to warm air through the warmer passage and blows out in the upper slope in winter. Thus, vent holes or openings in summer are specifically called cold wind-holes, while those in winter are called warm wind-holes (Aratani, 1926). It has been pointed out that the change of airflow between the cold and warm wind-holes takes place during April and October to November in most Japanese wind-holes.

The behavior of ^{222}Rn in underground caves in different geological materials has been studied throughout the world, e.g., solution cavities in the limestone of Alabama (Wilson et al., 1991), blowholes (another name for a wind-hole) in the Quaternary volcanic region of Spain (Baixeras et al., 2005; Monero et al., 2008, 2009), underground

* Corresponding author.
E-mail addresses: nomura@edu.shimane-u.ac.jp (R. Nomura), i247811@staff.kanazawa-u.ac.jp (M. Inoue), kofuji@jmsfmml.or.jp (H. Kofuji).

https://doi.org/10.1016/j.jenvrad.2018.12.008
Received 8 May 2018; Received in revised form 9 September 2018; Accepted 3 December 2018

quarries and coal mines (Perrier et al., 2004; Tchorz-Trzeciakiewicz and Parkitny, 2015), dead-end tunnels (Muramatsu et al., 2002; Richon et al., 2005; Perrier et al., 2007; Li et al., 2010) and tourism/non-tourism related caves (Dumitru et al., 2015). Those studies have shown that the ^{222}Rn concentrations were controlled by air flow generated by the underground-atmospheric temperature difference. Monero et al. (2009) also reported seasonal variations of ^{222}Rn concentrations, in which concentrations were 2.0–3.0 kBq/m^3 in summer and mostly under 0.1 kBq/m^3 in winter. Radon-222 emanation from soil or rock and subsequent diffusion are generally related to the regional geology, the parent radionuclide concentrations in source materials, and environmental factors such as temperature and wind conditions (Tanner, 1980; Nazaroff, 1992; Baixeras et al., 2005; Monero et al., 2008; Li et al., 2010; Sakoda et al., 2011; Pereira et al., 2017).

To the best of our knowledge, the ^{222}Rn concentrations in the air from the wind-hole of talus deposits have not been measured. Therefore, we measured the ^{222}Rn concentrations in the air blown from the Yakumo Wind-hole and found interesting seasonal variations. In this paper, we report on the results of the ^{222}Rn concentration analyses and discuss the mechanisms of the seasonal variation.

2. Geology of the Yakumo Wind-hole area

The Yakumo Wind-hole is located in Asahara, Sada Town, the southern part of Izumo City (lat. 35°14′34.39”N; long. 132°45′9.35”E). It is formed in the talus deposits distributed on the eastern side of Kuroyama Mountain, where a step showing a topographic indication of a large-scale landslip occurred on the middle slope of this mountain at elevations of 150–250 m a.s.l. The range in elevation of the talus deposits from the bottom to top is 170 m–215 m a.s.l., while its width is ~60 m at maximum (Figs. 1 and 2a). Rock boulders mostly ca. 30–50 cm in size are randomly distributed on the mountain slope (Fig. 2b), and the area outside of the talus is overlain by a saprophagous soil derived from fallen leaves.

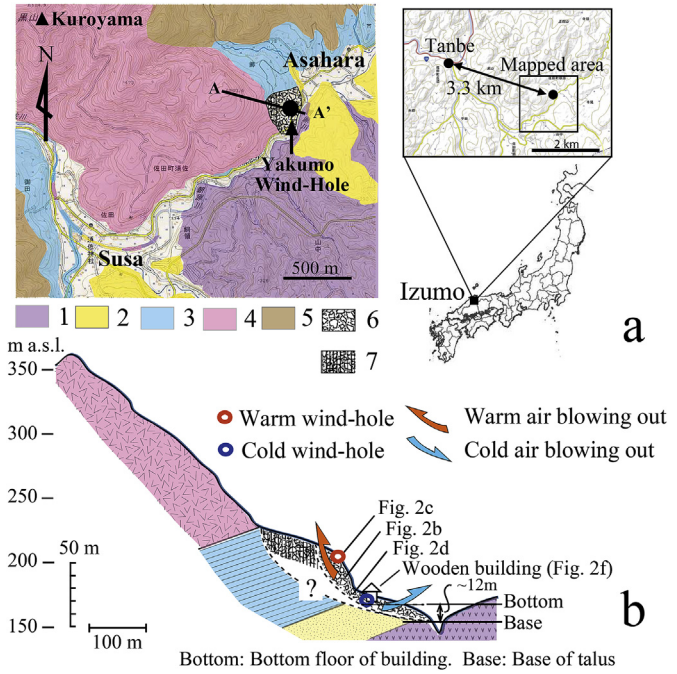

Fig. 1. Geological map showing the location of the talus deposits (a), and the cross-section of the Yakumo Wind-hole along line A–A' (b). 1, Andesite and its pyroclastics (Kawai Formation); 2, Sandstone (Kawai Formation); 3, Mudstone (Kuri Formation); 4, Rhyolite and its pyroclastics (Kuri Formation); 5, Andesite and its pyroclastics (Ohmori Formation); 6, Talus deposits; 7, Talus deposits covered with soil.

The geology of the Yakumo Wind-hole area consists of Miocene volcaniclastic and sedimentary rocks (Fig. 1), which belong to the Kuri Formation (Kano et al., 1998). A section of rhyolite of the Kuri Formation covers the mudstone in the southern part of Asahara. The combination of rhyolite overlying mudstone may have led to a topographically unstable steep slope that gave rise to the landslip in this area.

We measured the area ratio of rock boulders to void space, and we assumed that the inner structure of the talus deposits was comparable to the scattered rock boulders observable in the surface deposits. The void space was estimated to be 27% on average. This value seems reasonable, as the same values were recorded for void space in the cliff (Fig. 2d). The rock boulders are larger (30–100 cm) and more uneven in the upper talus, while they are smaller (5–30 cm) and less uneven in the lower talus.

The Yakumo Wind-hole is a tourist spot, and a wooden building is used to enable visitors to experience the cold, blowing air. The building is located on the ground at 170 m a.s.l., and it has three floors constructed below ground, with the bottom floor reaching to 8.5 m below ground level (Fig. 2f).

3. Methods

We carried out measurements of the ^{222}Rn concentrations, temperatures, and relative humidity (RH) levels on the bottom floor of the tourist facility (i.e., ~8.5 m below ground) (Fig. 2f), and on the top of the talus slope from February 2015 to the end of 2016. The measurement of temperature and relative humidity was further extended until the beginning of September 2017. The two observation points at the wooden building and at the location on the upper talus are hereafter referred to as the cold wind-hole (CWH) and warm wind-hole (WWH), respectively (Fig. 2e). We also referred to the atmospheric temperature measured by the regional government at Tanbe, Sada Town, which is 3.3 km northwest of Asahara, in order to investigate the critical atmospheric temperature that controls the blowing of air (Fig. 1a). The elevation difference between Asahara and Tanbe is 40 m.

We used two-sets of RAD7 radon detectors (Durridge, USA) for the ^{222}Rn measurements. A sampling tube was set about 30 cm inside the gap between the rocks at the WWH, and another was set about 20 cm above the 3rd basement floor of the building. Because no information had hitherto been obtained, we measured ^{222}Rn every hour in 2015 and every 2 h in 2016. The use of RAD7 in this investigation was effective because RAD7 separates ^{222}Rn (radon) and ^{220}Rn (thoron) signals and counts the two isotopes simultaneously with high sensitivities in such a way that the isotopes can be distinguished by the energies of their alpha particles (Durridge, 2018).

RAD7 is very sensitive to humidity. Radon-222 decayed positive ions such as ^{218}Po$^+$ create clusters of ions and water molecules. These clusters reduce the sensitivity in measurements (Durridge, 2018). Thus, in order to more effectively remove the moisture from the sample air, we used two-types of moisture exchanger (DRYSTIK ADS-3R and the 12-inch passive DRYSTIK, Durridge, USA) before the air entered the RAD7 measurement chamber. As a result, the relative humidity was reduced to below 10%, primarily between 7 and 9%.

Based on the two-sigma uncertainty, the analytical precision of ^{222}Rn was estimated as 1.3–57.3% (a mean of 4.1%) except for over 100% uncertainty in winter measurements with the low concentration. However, the measurement results with such a high uncertainty account for only 5.3%. Therefore, from the importance in our discussion, we used the ^{222}Rn data of all measurements.

For the measurements of temperature and relative humidity, Ondotori TR-73U Atmospheric Data Loggers (TandD, Japan) were used in the same locations that the ^{222}Rn was measured. The measuring sensors were as follows: a thermistor with a measurement accuracy of ± 0.3 °C for 0–50 °C and a polymer thin film sensor with a measurement accuracy of ± 5% RH for 10–95% RH.

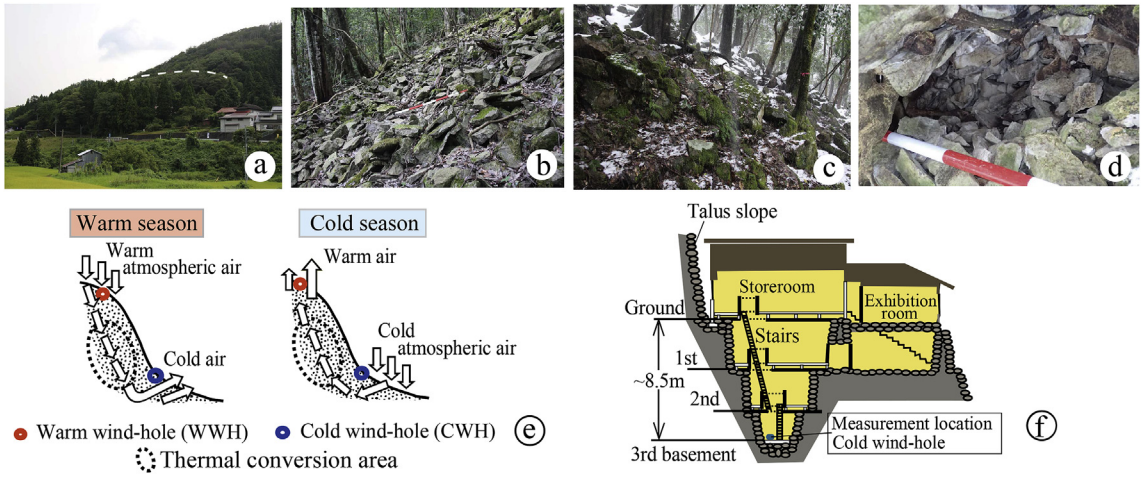

Fig. 2. a, Overview of the Yakumo Wind-hole. Broken line indicates the top of the talus deposits. b, Talus deposits with a scale bar of 120 cm c, The warm wind-hole at the time of snowfall. d, Internal view of the talus deposits with a scale bar graduated in 20 cm intervals. e, Convection model showing the blowing of cold wind in the warm season, which is contrasted with warm wind in the cold season, in response to the ambient atmospheric temperature. f, Sketch of the tourist facility in the Yakumo Wind-hole and the study site for the cold wind-hole.

4. Results

The ^{222}Rn concentrations at the CWH showed very similar seasonal variations during the two years of 2015 and 2016 (Fig. 3a). The blowing of air with remarkably high ^{222}Rn concentrations from the talus deposits began in early-middle May, and high concentrations of over 1.0 kBq/m^3 were mostly maintained in summer and early autumn; this was followed in October by near weekly remarkable fluctuations between 0.01 and 6.1 kBq/m^3. The highest concentration of 7.6 ± 0.1 kBq/m^3 was recorded in early September, while lower concentrations predominated from late October to early May of the next year, with intermittent high concentrations of 0.5–2.1 kBq/m^3.

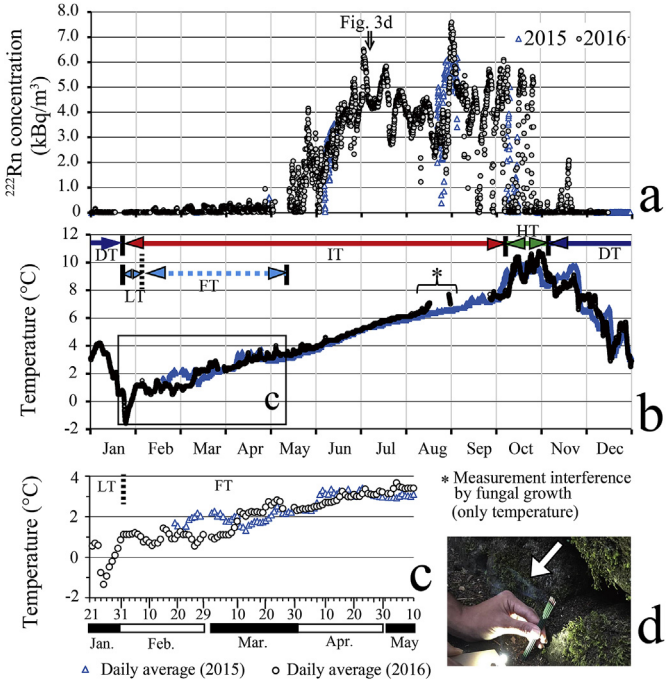

Fig. 3. Seasonal changes in ^{222}Rn concentrations (a) and temperature (b) throughout 2015 and 2016 at the cold wind-hole. Abbreviations indicate the time intervals characteristic of temperature variations. IT, Increasing temperature; DT, Decreasing temperature; HT, High temperature; LT, Low temperature; and FT, Fluctuated temperature. (c) Closeup of daily mean temperature showing intermittent temperature increase in the FT interval. (d) Smoke, indicated by the arrow, used to show the air blowing out at the cold wind-hole in early July 2016.

The CWH temperature changes showed almost the same pattern in both 2015 and 2016 (Fig. 3b). These changes were characterized by an increasing interval (IT) and a decreasing one (DT), with intercalation of a high temperature interval in October (HT). The increase in temperature began from early February and terminated at the earliest time in October. It should be noted that the temperature in the early IT of February to early May fluctuated (FT) with intermittent temperature increases of around 0.5 °C (Fig. 3c), but data were very stable in the latter half of the IT. It also should be noted that a rapid temperature increase of about 2.7 °C occurred after the end of the increasing interval (IT). The temperature decreasing interval (DT) was rather short, i.e., a total of 3 months from November to late January of the next year, and it transitioned to the lower temperature interval (LT) of late January to early February (Fig. 3b).

The ^{222}Rn concentrations at the WWH also showed seasonal variations (Figs. 4 and 5). They were low in summer, but occasional short-term concentrations as high as 2.6 kBq/m^3 were recorded at irregular intervals (Fig. 4a). The ^{222}Rn concentrations in winter were also low, i.e., mostly 0.02–0.06 kBq/m^3, although concentrations at the WWH were usually higher (a mean of ~0.05 kBq/m^3) than those at the CWH (a mean of ~0.02 kBq/m^3) (Fig. 5a). Although this difference may not be remarkable, the WWH characteristically lacks a covering of snow despite snowfall (Fig. 2c).

Aside from seasonal changes in the ^{222}Rn concentrations, the mean hourly concentrations during selected months in 2015 are displayed in Fig. 6 to allow for the examinations of the diurnal periodicities. The variation range indicated by the standard deviations of the ^{222}Rn concentrations was large in the warmer season (June, August–September) for both the CWH and WWH. The ^{222}Rn concentrations at the WWH showed an inverse relationship to the temperature in situ. In contrast, the CWH showed three different variation patterns in terms of the hourly concentrations associated with the WWH temperature increase; specifically, (1) the concentrations increased in June, (2) the concentrations decreased in December–January, and (3) high concentrations appeared in late morning before the daily temperature maximum in August–September.

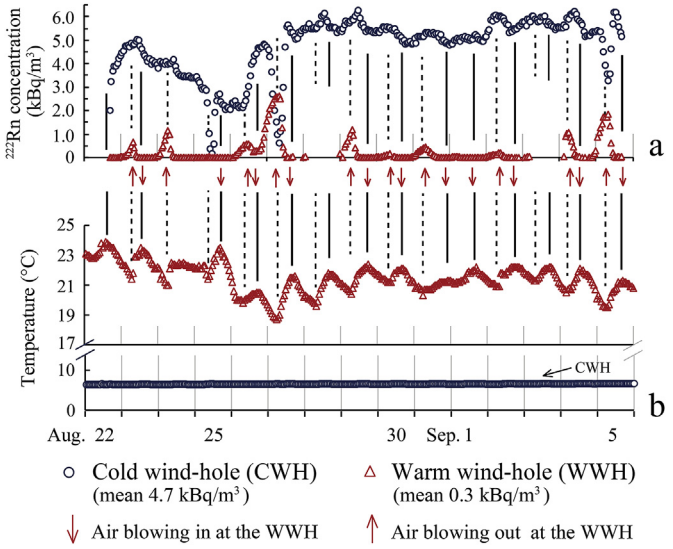

Fig. 4. Diurnal changes in ^{222}Rn concentrations and temperatures at the cold and warm wind-holes, during 22 August-6 September. Upward arrows indicate the estimated air flow with higher ^{222}Rn concentrations blowing out, while downward arrows indicate the estimated air flow with lower ^{222}Rn concentrations following suction. Solid and broken lines indicate the correlation lines of the temperature crest and trough to the fluctuations of ^{222}Rn concentrations, respectively. The mean ^{222}Rn concentration is the value of this interval.

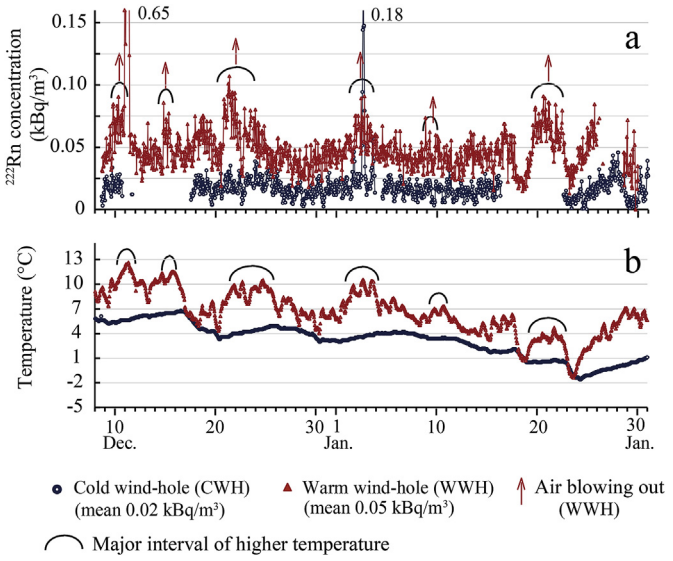

Fig. 5. Daily changes in ^{222}Rn concentrations at the cold wind-hole and warm wind-hole with respect to the temperature in December and January. Upward arrows indicate the major intervals of higher ^{222}Rn concentrations that correlate with the air with higher temperature blowing out at the warm wind-hole. The interval is indicated by the arch. The mean ^{222}Rn concentration is the value of this interval.

5. Discussion

5.1. ^{222}Rn at the CWH and WWH

High ^{222}Rn concentrations were recorded in summer at the CWH, while those at the WWH were low. Conversely, winter ^{222}Rn concentrations at the WWH were high, while those at the CWH were low. The summer and winter low levels of ^{222}Rn concentrations at each wind-hole were comparable to the local atmospheric levels in the Izumo Province (monthly concentrations: ~1.0–14.0 Bq/m^3; Yoshioka and Iida, 2007) and the prefectural area (a mean of 9.3 Bq/m^3; Oikawa et al., 2003) in many instances, except for instances when high concentrations occurred. Such low levels are indicative of the sucking of atmospheric air at each hole.

Reciprocal air flow between the CWH and WWH becomes prominent in summer and winter. According to the calculated heat exchange of air (Egawa et al., 1980) and tracer experimental results derived by using dry ice (CO_2 gas) (Tanaka et al., 2004), the flow speed between the WWH and CWH has been estimated to be a maximum of 2–3 cm/m during active summer convection. Although we did not measure the flow speed in the Yakumo Wind-hole, we could confirm that air was blowing out at a similar speed at the CWH in summer (Fig. 3d). The winter flow speed of air at the WWH has never been measured. In regard to our smoke examination results in winter, we could not perceive blowing at a measurable level.

A negative correlative relationship between the ^{222}Rn concentrations and temperatures at the WWH was detected in the warmer seasons (Fig. 4), which suggests that air with higher ^{222}Rn concentrations and lower temperatures blows out from the WWH at this time. Conversely, this is indicative of the sucking of summer atmospheric air with low ^{222}Rn concentrations and higher temperatures; higher temperature air always had low ^{222}Rn concentrations. In Figs. 4 and 5, the estimated wind directions at the WWH are shown with arrows (these data were based on the temperature difference between the CWH and WWH) along with the occurrences of higher ^{222}Rn concentrations. During winter temperature fluctuations, over a period of approximately 2–5 days, ^{222}Rn concentrations increased with the air temperature blowing out at the WWH, as indicated by the arches in Fig. 5. In this period during winter, the CWH temperature was always lower than that of the WWH. Thus, ^{222}Rn behavior with respect to temperature at the WWH was consistent with temperature-driven air convection throughout the year.

The ^{222}Rn behavior at the CWH, based on the air convection, was most clearly recognized around June. The data indicated the sucked warm air with low ^{222}Rn concentrations at the WWH blew out at the CWH, with a change to high concentrations (Fig. 6a). However, this relationship was complicated in summer. In many instances, relationships between the WWH temperature and the ^{222}Rn concentrations at the CWH were irregular, with positive, negative, and non-corresponding trends (Fig. 4). Unknown factors may still be involved in the talus deposit. It is significant that in August–September, ^{222}Rn concentrations showed a decreasing trend when the WWH sucked high temperature air (Fig. 6b). Variations in ^{222}Rn concentrations were not always related to temperature alone in the warmest season, which required that we assess the relationship to humidity.

5.2. Increasing and decreasing conditions of higher ^{222}Rn concentrations at the CWH

Radon-222 concentrations at the CWH were low for almost every day in April, but values increased to over ~1.0 kBq/m^3 by mid-May over a short period of time, although we were missing 11 days of data because of battery trouble (Fig. 7a). When the daily ^{222}Rn concentrations during April–May were plotted against the daily mean atmospheric temperature at Tanbe (Fig. 8a), we were able to classify the data into two groups with different slopes by the threshold temperature of 16.2 °C, which was determined by the intersection point with the two regression lines, ranging 8.8–16.1 °C and 0.03–0.3 kBq/m^3 (r = 0.68), and 16.6–22.0 °C and 0.2–3.5 kBq/m^3 (r = 0.78), respectively. The threshold temperature may be critical for the beginning of steady-state downward air convection, i.e., the air blows out from the CWH over this temperature.

In October, high concentrations of over ~3.0 kBq/m^3 continued when the atmospheric temperature at Tanbe was maintained largely at the values greater than ~18 °C (Fig. 7b). When the temperature was less than ~18 °C, the ^{222}Rn concentrations tended to decrease and they

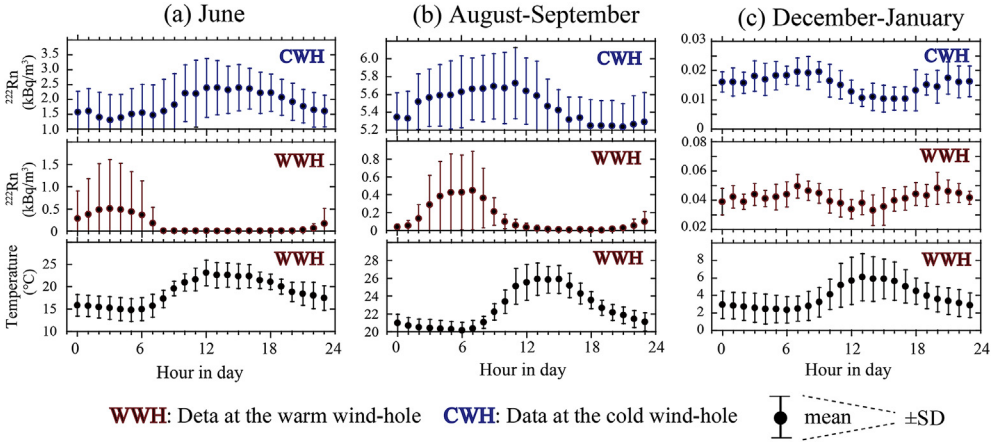

Fig. 6. Hourly changes in ^{222}Rn concentrations at the cold wind-hole and warm wind-hole correlated with the temperature at the warm wind-hole during major periods of 2015. The results are given as a (a) 6 day summary in June; (b) 8 day summary from August to September (same data source of Fig. 4, except for abnormal values); and (c) 11 day summary from December to January (same data source of Fig. 5, except for abnormal values). SD, standard deviation.

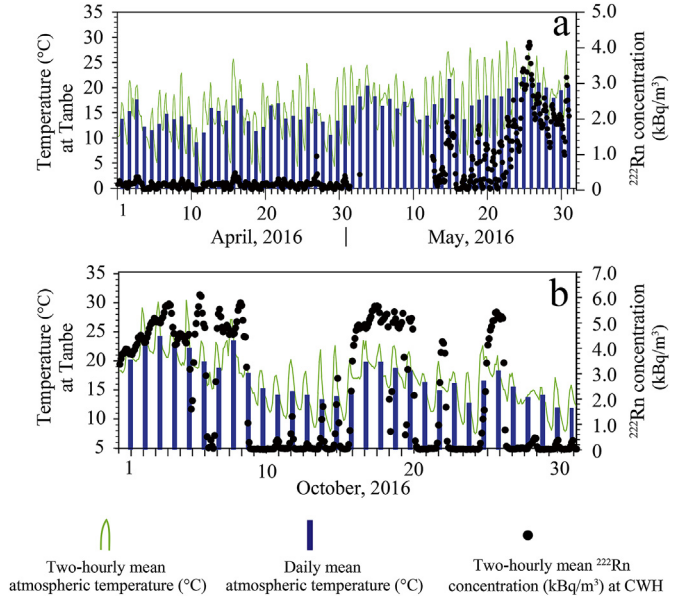

Fig. 7. Radon-222 concentrations and atmospheric temperature changes every 2 h in the periods of increasing (a) and decreasing (b) radon-rich air at the cold wind-hole. Bar graph shows the mean temperature of the day. Atmospheric temperature was measured at Tanbe.

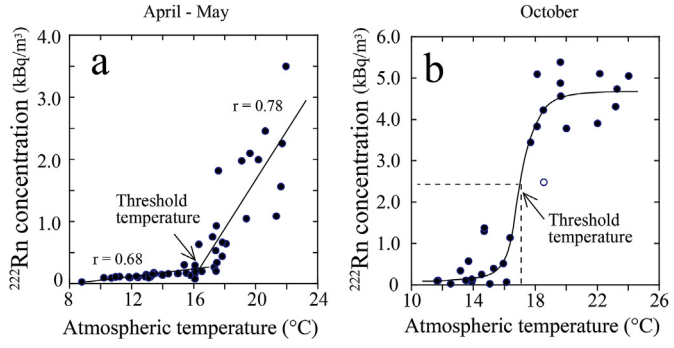

Fig. 8. Correlation between ^{222}Rn concentrations at the cold wind-hole and atmospheric temperature at Tanbe. (a) The increasing period of April–May contains two groups represented by different regression lines with an intersection point of 16.2 °C. (b) The decreasing period of October with two groups represented by a sigmoid function with an inflection point at 17.1 °C, except for the outlier (open circle). Each ^{222}Rn concentration and temperature data point represents daily averaged data.

were mostly very low at values less than ~0.5 kBq/m^3 when the mean temperature during the day was less than ~14 °C. The plotting of the daily ^{222}Rn concentrations against the daily mean atmospheric temperature at Tanbe (Fig. 8b) revealed that the ^{222}Rn concentrations depended on the atmospheric temperature, as represented by a sigmoid function. The sigmoid function, if one datum (18.6 °C, 2.5 kBq/m^3) is regarded as outlying point, best describes the inflection point at 17.1 °C (r^2 = 0.94, the residual errors normally distributed with p = 0.17 > 0.05 (significance level) by Shapiro-Wilks test in a three parameter nonlinear regression analysis; SigmaPlot version 12.5, www.systatsoftware.com.). This temperature corresponded to 2.4 kBq/m^3 and was associated with the forming of a phase-out of major ^{222}Rn diffusion below this temperature.

The beginning and ending of active air blowing with higher ^{222}Rn concentrations at the CWH were reflected in the atmospheric temperature, but the ^{222}Rn diffusing ability against the atmospheric temperature was different. Referring to the case of Italian blowholes, the critical atmospheric temperature was founded to be 15 °C for the transition from 1.0 to 2.0 kBq/m^3 (Moreno et al., 2009). The threshold temperature of the Yakumo Wind-hole was somewhat higher in both spring and autumn.

5.3. High ^{222}Rn concentrations in warmer seasons and the effect of water

Convection theory explains that outside air is drawn into the wind-hole where it can exchange heat by making contact with rocks or ice, and by mixing with the inside air through the passages in the talus, whereby air with a changed temperature blows out (Aratani, 1923, 1926; Egawa et al., 1980; Tanaka et al., 2000a, 2000b; 2004, 2006; Byun et al., 2011).

Water vapor during the heat exchange is a critical factor for the behavior of ^{222}Rn, as repeatedly pointed out in studies on ^{222}Rn emanations (Tanner, 1980; Strong and Levins, 1982; Stranden et al., 1984; Nazaroff, 1992; Menetrez et al., 1996; Schumann and Gundersen, 1996; Barillon et al., 2005; Breitner et al., 2010; Hassan et al., 2011; Arvela et al., 2016). We measured the relative humidity in the CWH from March 2015 to May 2017. As shown in Fig. 9, relative humidity at the CWH was determined to be very high throughout the year, except for the decrease in winter. High humidity, such as values over 95%, in the warmer seasons exceeded the measurable value by the sensor, but the lowered humidity in winter and early spring, decreased to 80–90%; similar data were also previously reported by Ogawa (1996).

It has been pointed out, from the viewpoint of the behavior of ^{222}Rn atoms in the microspace of materials, that liquid water and temperature are two factors that play an important role in the processes of ^{222}Rn emanation and exhalation (Tanner, 1980; Nazaroff, 1992). The presence of water among grains directly influences the ^{222}Rn emanation from radium-bearing rocks, diffusion and convection in air, and

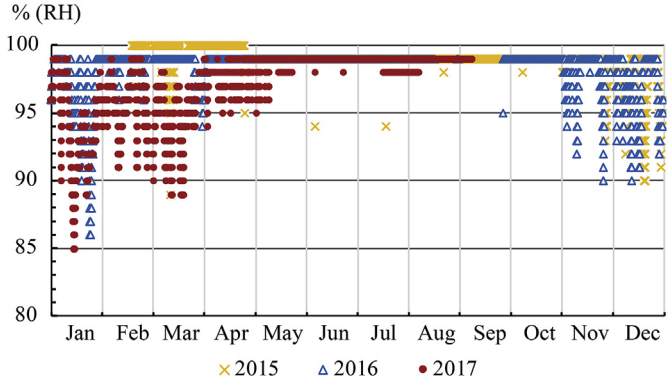

Fig. 9. Monthly changes in relative humidity at the cold wind-hole.

adsorption on surrounding mineral grains (Tanner, 1980; Nazaroff, 1992; UNSCEAR, 2000). Experimental results show that ^{222}Rn adsorption on soil grains decreases rapidly with increasing water content and becomes insignificant for water contents greater than about 0.3–0.4 of saturation (UNSCEAR, 2000). Thus, if ^{222}Rn is trapped in water, less ^{222}Rn is available in the gas phase. It also has been pointed out that significant proportions of ^{222}Rn can be considered to be trapped in the water phase of soil (Washington and Rose, 1990; Schumann and Gundersen, 1996). The ^{222}Rn solubility in water, which follows the Ostwald coefficient, decreases with increasing temperature (UNSCEAR, 2000). The optimal value of ^{222}Rn diffusion may change with the water content in different samples.

This information supports our observations at the CWH that high concentrations of ^{222}Rn occurred during the relatively high humidity season of early summer to August, and in contrast, lower ^{222}Rn concentrations occurred in the lower humidity season of winter and early spring. Therefore, it is clear that the ^{222}Rn behavior in the talus depends on the activity of blowing air in combination with the relative humidity.

Despite the high temperatures and high humidity of the summer season, some intervals ranging from 2 to 5 days with decreased ^{222}Rn concentrations occurred in late July to August (Fig. 3a). After the end of these decreased intervals, the highest ^{222}Rn concentration of 7.6 kBq/m^3 occurred in early September, which was near the maximum CWH temperature. These phenomena may be interpreted to have occurred under the following two conditions. (1) The ^{222}Rn-rich air flowing within the talus decreased at the CWH because the air moved up to blow out at the WWH, and (2) there was a combination of increasing volumes of cold water and subsequent increases in the ^{222}Rn solubility in the water. In the case of (1), as can be seen in August 22–27 in Fig. 4, short-term changes of the ^{222}Rn concentrations within one day occurred at the CWH, and the ^{222}Rn concentrations at the WWH responded in various ways to that at the CWH as stated before. In regard to the decreases ranging from two or three days, however, no clear correlations were recognized. This interpretation thus can not be accepted. In the case of (2), we can assume that wet conditions formed in some places in the interior of the talus. If there was some volume of cold meltwater and the ^{222}Rn was trapped in it, the diffusion potential of ^{222}Rn from the inside of the talus would consequently be decreased. Furthermore, if we assume that the water with abundant dissolved ^{222}Rn produces high vapor, then a greater amount of ^{222}Rn would be released. This may have been the case for the highest ^{222}Rn concentrations in early September. In consequence, ^{222}Rn diffusion from the wind-hole is dependent on what phase of water has formed on the rock boulders during the convective processes. This hypothesis requires verification in the future.

5.4. Potential ice inside the talus deposits

It is a significant issue as to whether ice is formed or not in the interior of the talus, which could contribute to the blowing of cold air during the warmer season. Ice can be considered as the major driving force promoting convection in the talus. Previous reports have suggested that ice is formed inside talus in various wind-holes in Japan, e.g., Hokkaido (Shiboi, 1974; Sawada, 2003; Sawada et al., 2003), prefectures of Akita (Aratani, 1923, 1926), Miyagi (Egawa et al., 1980), and Fukushima (Tanaka et al., 2000b), as well as in Korea (Tanaka et al., 2000a, 2006; Byun et al., 2011). Among the recent observations on ice in the talus, it is noted that ice grows not in winter, but in spring. Sawada (2003) and Sawada et al. (2003) observed that meltwater from snow in spring flowed into deeper places and refroze on the perennial ice until the middle of April, despite mean annual air temperatures of over 0 °C. He also suggested that the ice continued melting during the summer to early autumn. Similarly, ice does not grow in winter, but during the late spring to early summer at the Ice Valley in Korea (Byun et al., 2011). Numerical simulations revealed that the hotter the outside air is, the larger the ice growth is in spring (Tanaka et al., 2006). We also observed rock boulders covered with clear ice in the talus in the early to middle of March. We consider that the mechanism of ice generation is similar to that of freezing rain, which is controlled by the saturated water vapor pressure around ice, at an air temperature below the freezing point. The intermittent increase of temperature in the FT interval (Fig. 3c) would have contributed to the growth of ice. Taking these observations and the simulations into consideration, we conclude that the Yakumo Wind-hole is associated with ice as a cooling mechanism in the warmer seasons from spring to autumn.

The seasonal variation of ^{222}Rn behavior can be reasonably explained by ice formation and melting processes. Atmospheric temperatures of ~20 °C appeared repeatedly in late March to early May, but the ^{222}Rn concentrations at the CWH were still very low (Fig. 7a). This can be explained by the diffusing ^{222}Rn becoming trapped in meltwater that refreezes to form more ice. Consistently, the CWH air temperature gradually increased from ~3 to ~8 °C from mid-May to early September (IT interval of Fig. 3b), which should correspond to intervals of ice melting, thus making it impossible for the ice to refreeze. Abrupt increases (from 7.4 °C to 10.3 °C in 6 days) in the CWH air temperature in early October (Fig. 3b) indicate the disappearance of the ice inside the talus. Thus, 4.5 months (from middle May to end of September) were needed to melt the ice.

6. Conclusion

This was the first attempt to interpret the interior conditions of an algific talus in terms of the behavior of ^{222}Rn throughout the year. Our conclusions are as follows:

(1) In the warm season, cold air with high ^{222}Rn concentrations (maximum 7.6 ± 0.1 kBq/m^3) blew out at the CHW, in contrast to the warm air with low ^{222}Rn concentrations that blew into the WWH. In the cold season, the air flow and the concentrations at the CWH were reverse to those in the warm season. The ^{222}Rn concentrations at these wind holes showed a clear seasonal variation.
(2) Air with high ^{222}Rn concentrations actively blew out from the CWH when the daily atmospheric temperature at Tanbe (as the representative location for the regional atmospheric temperature) constantly exceeded a value of over 16.2 °C, and the ^{222}Rn concentrations abated when the temperature was less than 17.1 °C, which suggests that there is a threshold temperature for the convection.
(3) High ^{222}Rn concentrations in mid-May to October were correlated with the interval of high humidity. We pointed out two hypotheses concerning a^{222}Rn trap; one involves ^{222}Rn dissolution in meltwater in the warmest season (late July to August), and the other involves the ^{222}Rn trap in growing ice in spring. The former refers to high ^{222}Rn solubility in cold water that results in less ^{222}Rn in the gas phase, and the latter is based on the observed information showing

that ice can also grow in the warm season.

Since the Yakumo Wind-hole is also a tourist facility, it would be worthwhile to conduct future research investigating the impacts of ^{222}Rn exposures on the health of tourists and guides.

Acknowledgements

We are deeply indebted to members of the Fhutaro-no-kai, the administrative organization of the Yakumo Wind-hole, particularly Chairman H. Katsube, and to the Izumo Provincial Office of the Shimane Prefectural Government for the provisioning of temperature data. This work was supported by a Japanese Grant-in Aid for Scientific Research (C) (R. Nomura, No. 17K02110).

Appendix A. Supplementary data

Supplementary data related to this article can be found at https://doi.org/10.1016/j.jenvrad.2018.12.008.

References

Aratani, T., 1923. Katayama wind-hole, Akita prefecture. J. Geogr. 36, 732–738 (in Japanese).
Aratani, T., 1926. On the Nagahashiri wind-hole, Akita prefecture. Chikyu 8, 426–441 (in Japanese).
Arvela, H., Holmgren, O., Hänninen, P., 2016. Effect of soil moisture on seasonal variation in indoor radon concentration: modelling and measurements in 326 Finnish houses. Radiat. Protect. Dosim. 168, 277–290.
Baixeras, C., Bach, J., Amgaroua, K., Morenoa, V., Fonta, L., 2005. Radon levels in the volcanic region of La Garrotxa, Spain. Radiat. Meas. 40, 509–512.
Barillon, R., Özgümüs, A., Chambaudet, A., 2005. Direct recoil radon emanation from crystalline phases. Influence of moisture content. Geochem. Cosmochim. Acta 69, 2735–2744.
Breitner, D.H., Arvela, H., Hellmuth, K.-H., Renvall, T., 2010. Effect of moisture content on emanation at different grain size fractions - a pilot study on granitic esker sand sample. J. Environ. Radioact. 10, 1002–1006.
Byun, H.-R., Tanaka, H.L., Choi, P.-Y., Kim, D.-W., 2011. Seasonal reversal at miryang eoreumgol (Ice Valley), Korea: observation and monitoring. Theor. Appl. Climatol. 106, 403–415.
Dumitru, O.A., Onac, B.P., Fornós, J.J., Constantin Cosma, C., Ginés, A., Ginés, J., Merino, A., 2015. Radon survey in caves from mallorca Island, Spain. Sci. Total Environ. 526, 196–203.
Durridge, 2018. RAD7. User manual. Available at: https://durridge.com/documentation/RAD7%20Manual.pdf .
Egawa, Y., Hori, N., Sakayama, T., 1980. On the cause of the subsurface cold air circulation at debris accumulated slopes. J. Geogr. 89, 85–96 (in Japanese with English abstract).
Hassan, N., Ishikawa, T., Hosoda, M., Iwaoka, K., Sorimachi, A., Sahoo, S., Janik, M., Kranrod, C., Yonehara, H., Fukushi, M., Tokonami, S., 2011. The effect of water content on the radon emanation coefficient for some building materials used in Japan. Radiat. Meas. 46, 232–237.
Kano, K., Matsuura, H., Sawada, Y., Takeuchi, K., 1998. Geology of the Iwami-oda and Oura Districts. With Geological Sheet Map at 1:50,000. Geol. Surv. Japan, pp. 118p (in Japanese with English abstract).
Li, X., Song, B., Zheng, B., Wang, Y., Wang, X., 2010. The distribution of radon in tunnels with different geological characteristics in China. J. Environ. Radioact. 101, 345–348.
Maki, T., 1998. Characteristics of topograph, climate and vegatation around Jagaraamogara wind cave basin. J. Agric. Meteorol. 54, 255–266 (in Japanese with English abstract).
Menetrez, M.Y., Mosley, R.B., Snoddy, R., Brubaker Jr., S.A., 1996. Evaluation of radon emanation from soil with varying moisture content in a soil chamber. Environ. Int. 22, s447–s453.
Moreno, V., Baixeras, C., Font, L., Bach, J., 2008. Indoor radon levels and their dynamics in relation with the geological characteristics of La Garrotxa, Spain. Radiat. Meas. 43, 1532–1540.
Moreno, V., Bach, J., Baixeras, C., Font, L., 2009. Characterization of blowholes as radon and thoron sources in the volcanic region of La Garrotxa, Spain. Radiat. Meas. 44, 929–933.
Muramatsu, H., Tashiro, Y., Hasegawa, N., Misawa, C., Minami, M., 2002. Seasonal variations of ^{222}Rn concentrations in the air of a tunnel located in Nagano City. J. Environ. Radioact. 60, 263–274.
Nazaroff, W.W., 1992. Radon transport from soil to air. Rev. Geophys. 30, 137–160.
Ogawa, H., 1996. Annual fluctuation of temperature and its factors in Yakumo Fuketsu (wind cavity), Sada Town, Shimane prefecture. Shimane Chirigakkaishi (J. Shimane Geogr. Assoc.) 32, 35–46.
Oikawa, S., Kanno, N., Sanada, T., Ohashi, N., Uesugi, M., Sato, K., Abukawa, J., Higuchi, H., 2003. A nationwide survey of outdoor radon concentration in Japan. J. Environ. Radioact. 65, 203–213.
Pereira, A., Lamas, R., Miranda, M., Domingos, F., Neves, L., Ferreira, N., Costa, L., 2017. Estimation of the radon production rate in granite rocks and evaluation of the implications for geogenic radon potential maps: a case study in Central Portugal. J. Environ. Radioact. 166, 270–277.
Perrier, F., Richon, P., Crouzeix, C., Morat, P., Le Mouël, J.L., 2004. Radon-222 signatures of natural ventilation regimes in an underground quarry. J. Environ. Radioact. 71, 17–32.
Perrier, F., Richon, P., Gautam, U., Tiwari, D.R., Shrestha, P., Sapkota, S.N., 2007. Seasonal variations of natural ventilation and radon-222 exhalation in a slightly rising dead-end tunnel. J. Environ. Radioact. 97, 220–235.
Richon, P., Perrier, F., Sabroux, J.C., Trique, M., Ferry, C., Voisin, V., Pili, E., 2005. Spatial and time variations of radon-222 concentration in the atmosphere of a dead-end horizontal tunnel. J. Environ. Radioact. 78, 179–198.
Sakoda, A., Ishimori, Y., Yamaoka, K.A., 2011. Comprehensive review of radon emanation measurements for mineral, rock, soil, mill tailing and fly ash. Appl. Radiat. Isot. 69, 1422–1435.
Sawada, Y., 2003. Monitoring of ground-ice formation in a block slope at Mt. Nishi-Nupukaushinupuri, Hokkaido, Japan. Proc. 8th Int. Conf. Permafrost, Zurich, Switzerland 2, 1001–1005.
Sawada, Y., Ishikawa, M., Ono, Y., 2003. Thermal regime of sporadic permafrost in a block slope on Mt. Nishi-Nupukaushinupuri, Hokkaido Island, Northern Japan. Geomorphology 52, 121–130.
Sawada, Y., 2015. The mechanism of Fhuketsu. In: Shimizu, C., Sawada, Y. (Eds.), Ice Caves, Algific Talus Slopes and Natural Cold Storage in Japan. Kokon-Shoin Plub., Tokyo), pp. 23–40 (in Japanese).
Schumann, R.R., Gundersen, L.C.S., 1996. Geologic and climatic controls on the radon emanation coefficient. Environ. Int. 22, S439–S446.
Shimizu, C., 2004. Data base of Japanese wind-holes: in relation to geography, permafrost, and so on. Komazawa Geogr 40, 121–148 (in Japanese).
Shimizu, C., 2015. Japanese fhuketsu. In: Shimizu, C., Sawada, Y. (Eds.), Ice Caves, Algific Talus Slopes and Natural Cold Storage in Japan. Kokon-Shoin Plub., Tokyo, pp. 1–22 (in Japanese).
Shiboi, T., 1974. On the subsurface cold air circulation observed at Onneyu-Tsutsujiyama, Rubeshibe-cho, Hokkaido. J. Geogr. 83, 89–102 (in Japaese with English abstract).
Stranden, E., Kolstad, A.K., Lind, B., 1984. The influence of moisture and temperature on radon exhalation. Radiat. Protect. Dosim. 7, 55–58.
Strong, K.P., Levins, D., 1982. Effect of moisture content on radon emanation from uranium ore and tailings. Health Phys. 42, 27–32.
Tanaka, H.L., Nohara, D., Yokoi, M., 2000a. Numerical simulation of wind hole circulation and summertime ice formation at Ice Valley in Korea. J. Meteorol. Soc. Japan 78, 611–630.
Tanaka, H.L., Yokoi, M., Nohara, D., 2000b. Observational study of summertime ice at the Nakayama wind-hole in Shimogo, Fukushima. Sci. Rep., Inst. Geosci., Univ. Tsukuba, sec. A (Geol. Sci.) 21, 1–21.
Tanaka, H.L., Mura, N., Nohara, D., 2004. Mechanism of cold air vent at the Nakayama wind-hole in Shimogo, Fukushima. Geogr. Rev. Jpn. 77, 1–18 (in Japanese with English Abstract).
Tanaka, H.L., Nohara, D., Byun, H.-R., 2006. Numerical simulation of wind hole circulation at Ice Valley in Korea using a simple 2D model. J. Meteorol. Soc. Japan 84, 1073–1084.
Tanner, A.B., 1980. Radon migration in the ground. A supplementary review. In: In: Gesell, T.F., Lowder, W.M. (Eds.), Natural Radiation Environment III, vol. 1. pp. 5–56.
Tchorz-Trzeciakiewicz, D.E., Parkitny, T., 2015. Radon as a tracer of daily, seasonal and spatial air movements in the underground tourist route “Coal Mine” (SW Poland). J. Environ. Radioact. 149, 90–98.
United Nations Scientific Committee on the Effects of Atomic Radiation (UNSCEAR), 2000. Sources and Effects of Ionizing Radiation Vol. I: Sources United Nations Publications, New York.
Washington, J.W., Rose, A.W., 1990. Regional and temporal relations of radon in soil gas to soil temperature and moisture. Geophys. Res. Lett. 17, 829–832.
Wilson, D.L., Gammage, R.B., Dudney, C.S., Saultz, R.J., 1991. Summertime elevation of ^{222}Rn levels in Huntsville, Alabama. Health Phys. 60, 189–197.
Yoshioka, K., Iida, T., 2007. Major factors influencing long-term periodic variation of the radon concentration in the atmosphere: a comparative study between the ocean and land conditions. Jpn. J. Health Phys. 42, 53–62 (in Japanese with English abstract).